後頚部両側に発生し，異なるMRI所見を呈した spindle cell lipomaの1例

滑川陽一[1)~3)]，小林英介[1)]，藤原智洋[1)]，丹澤義一[1)]，川井　章[1)]，中馬広一[1)]

Spindle cell lipoma（以下SCL）は全脂肪細胞腫瘍の1.5%を占める比較的稀な腫瘍である．今回，我々は後頚部にSCLが両側発生し，異なるMRI所見を呈した非常に稀な1例を経験したので報告する．

症　　例

57歳，男性．主訴は2つの後頚部腫瘤．既往歴，家族歴に特記すべき事項なし．初診時の10年前より頚部に母指頭大の腫瘤を自覚していたが，徐々に増大傾向を認めたため，当院を受診した．初診時に頚部の左右両側皮下に腫瘤を認めた（図1）．右頚部腫瘤は5×4cm大で弾性硬，左頚部腫瘤は4×4cm大の軟らかい腫瘤で，ともに可動性は良好であった．

術前MRIでは，両腫瘤に連続性は認めず，右頚部腫瘤はT1で筋肉よりやや高信号，T2で高信号，ガドリニウムで不均一に造影された．一方で，左頚部腫瘤はT1で筋肉と等信号，T2で高信号，ガドリニウムでは造影されなかった（図2）．

切除生検にて右頚部腫瘤はSCLと診断され，また左頚部腫瘤は画像上lipomaが疑われたため，いずれの腫瘍にも辺縁切除を行った．

病理組織所見ではいずれの腫瘍でも紡錘形腫大核を有する腫瘍細胞が繊細な膠原線維の増生を伴って増殖しており，脂肪組織の混在も認めた（図3a，b）．免疫組織染色では，両腫瘍で紡錘形細胞がCD34に陽性を示し，ともにSCLと診断された（図3c，d）．組織学的には右頚部腫瘍が脂肪成分に乏しいいわゆるlow-fat type SCLであったのに対し，左頚部腫瘍は脂肪成分に富んだSCLであった．術後経過は良好で，両腫瘍ともに術後5年の現在，再発を認めていない．

図1　症例．57歳男性　2つの後頚部腫瘍を認める．

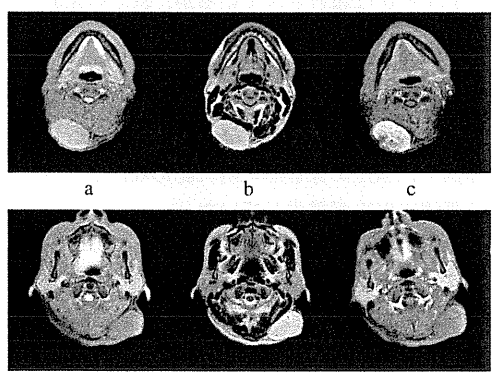

a　b　c　d　c　f

図2　右頚部腫瘍　a　T1強調　b　T2強調　c　Gd造影　左頚部腫瘍　d　T1強調　e　T2強調　f　Gd造影

考　　察

SCLはEnzingerらによって1975年に提唱されたlipomaの一亜型で，40～60歳代の中年男性の肩，頚

A case report of bilateral cervical spindle cell lipomas with different MRI findings : Yoichi NAMEKAWA et al. (Department of Musculoskeletal Oncology, National Cancer Center Hospital)

1）国立がん研究センター中央病院骨軟部腫瘍科　2）東京女子医科大学整形外科学教室　3）牛久愛和総合病院整形外科

Key words : Spindle cell lipoma, Bilateral, Low-fat spindle cell lipoma

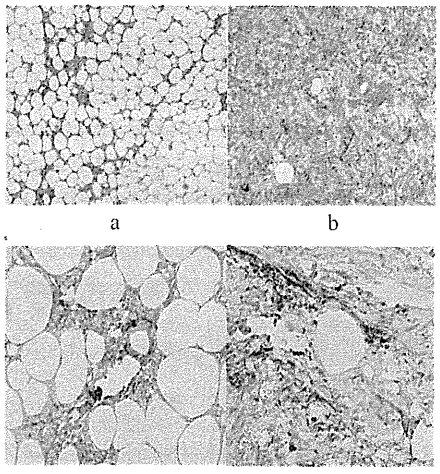

a　　b

c　　d

図3　HE染色　a：左頚部腫瘍　b：右頚部腫瘍，CD34染色　c：左頚部腫瘍　d：右頚部腫瘍

部，上背部に好発することが知られている[1]．SCLが多発する例は報告されているが，SCLの家族歴のない場合にSCLが多発する例は稀であり，われわれの渉猟しえた限りでは過去に13例のみであった[2]．中でも同一部位の両側にSCLが発生した例は過去に3例（胸壁，肩，舌）のみと極めて稀であった[2]．本症例ではSCLの家族歴は特に認めなかったが，後頚部両側にSCLが発生していた．

SCLには組織学的に脂肪細胞の割合によるvariantが存在することが知られており，脂肪細胞の割合が5％以下のlow-fat typeや脂肪細胞を欠いているfat-free typeが報告されている[3]．Sachdevaらは38例のSCLを検討した結果，うち5例で脂肪細胞の割合が5％以下であるlow-fat SCLであったと報告し，2例では脂肪細胞を認めないfat-free SCLであったと報告している[3]．またMRI所見でもSCLは細胞成分の割合によって多彩な像をとりうることが報告されている[4]．これらの理由により，しばしばSCLは画像上での他の腫瘍との鑑別が困難であるとされている．

本症例においても後頚部に認められた2つのSCLで組織学的に脂肪成分の割合が大きく異なっており，MRIで異なる画像所見を呈したために，術前の診断は困難であった．多彩な画像所見を呈しうることから，切除標本から慎重にSCLを診断する必要があると考えられた．

ま　と　め

後頚部の両側に発生し，異なるMRI所見を呈した極めて稀なspindle cell lipomaの1例を報告した．

文　　献

1) Enzinger FM, Harvey DA. Spindle cell lipoma. Cancer　1975；36：1852-1859.
2) Fanburg-Smith JC, Devaney KO, Miettinen M, et al. Multiple spindle cell lipomas: a report of 7 familial and 11 nonfamilial cases. Am J Surg Pathol　1988；22：40-48.
3) Sachdeva MP, Goldblum JR, Rubin BP, et al. Low-fat and fat-free pleomorphic lipomas: a diagnostic challenge. Am J Dermatopathol　2009；31：423-426.
4) Bancroft LW, Kransdorf MJ, Peterson JJ, et al. Imaging characteristics of spindle cell lipoma. AJR Am J Roentgenol　2003；181：1251-1254.

STEM CELLS®

CANCER STEM CELLS

Clinical Relevance and Therapeutic Significance of microRNA-133a Expression Profiles and Functions in Malignant Osteosarcoma-Initiating Cells

TOMOHIRO FUJIWARA[1, 5, 6], TAKESHI KATSUDA[1], KEITARO HAGIWARA[1], NOBUYOSHI KOSAKA[1], YUSUKE YOSHIOKA[1], RYOU-U TAKAHASHI[1], FUMITAKA TAKESHITA[1], DAISUKE KUBOTA[2], TADASHI KONDO[2], HITOSHI ICHIKAWA[3], AKIHIKO YOSHIDA[4], EISUKE KOBAYASHI[5], AKIRA KAWAI[5], TOSHIFUMI OZAKI[6], TAKAHIRO OCHIYA[1]

[1]Division of Molecular and Cellular Medicine, National Cancer Center Research Institute, Tokyo, Japan; [2]Division of Pharmacoproteomics, National Cancer Center Research Institute, Tokyo, Japan; [3]Division of Cancer Transcriptome Project, National Cancer Center Research Institute, Tokyo, Japan; [4]Department of Pathology and Clinical Laboratories, National Cancer Center Hospital, Tokyo, Japan; [5]Department of Musculoskeletal Oncology, National Cancer Center Hospital, Tokyo, Japan; [6]Department of Orthopedic Surgery, Okayama University Graduate School of Medicine, Dentistry, and Pharmaceutical Sciences, Okayama, Japan

Key words. Osteosarcoma • miRNA • Locked nucleic acid (LNA) • Clinical translation

ABSTRACT

Novel strategies against treatment-resistant tumor cells remain a challenging but promising therapeutic approach. Despite accumulated evidence suggesting the presence of highly malignant cell populations

Author contributions: T.F.: performed the experimental work, data analysis and writing of the draft of the manuscript; T.K., K.H.: and Y.Y.: provided the technical skills for the *in vitro* assay; N.K.: and R.T.: participated in the conception, design and coordination of the study; F.T.: provided the technical skills for the *in vivo* LNA delivery; D.K., I.K., A.Y.: and E.K.: provided osteosarcoma biopsy samples and their information; H.I.: provided osteosarcoma cell lines from clinical samples resected at the National Cancer Center Hospital of Japan; A.K.: and T.O.: initiated the project and provided helpful discussion. The manuscript was finalized by T.O.: with the assistance of all authors.

Correspondence should be addressed to Takahiro Ochiya: 5-1-1, Tsukiji, Chuo-ku, Tokyo 104-0045, Japan Phone: +81-3-3542-2511 (Ex. 4800); Fax: +81-3-5565-0727; e-mail: tochiya@ncc.go.jp; Received July 08, 2013; accepted for publication November 22, 2013; available online without subscription through the open access option. 1066-5099/2013/$30.00/0 doi: 10.1002/stem.1618

This article has been accepted for publication and undergone full peer review but has not been through the copyediting, typesetting, pagination and proofreading process which may lead to differences between this version and the Version of Record. Please cite this article as doi: 10.1002/stem.1618

within tumors, the unsolved issues such as *in vivo* targeting and clinical relevance remain. Here, we report a preclinical trial based on the identified molecular mechanisms underlying osteosarcoma-initiating cells and their clinical relevance. We identified key microRNAs (miRNAs) that were deregulated in a highly malignant CD133^{high} population and found that miR-133a regulated the cell invasion that characterizes a lethal tumor phenotype. Silencing of miR-133a with locked nucleic acid (LNA) reduced cell invasion of this cell population, and systemic administration of LNA-antimiR-133a along with chemotherapy suppressed lung metastasis and prolonged the survival of osteosarcoma-bearing mice. Furthermore, in a clinical study, high expression levels of CD133 and miR-133a were significantly correlated with poor prognosis, whereas high expression levels of the four miR-133a target genes were correlated with good prognosis. Overall, silencing of miR-133a with concurrent chemotherapy would represent a novel strategy that targets multiple regulatory pathways associated with metastasis of the malignant cell population within osteosarcoma.

INTRODUCTION

Sarcomas are distinctly heterogeneous tumors [1, 2]. Although the origin of sarcomas remains unknown, the overwhelming number of histopathological types and subtypes implies that sarcomas are a 'stem cell malignancy' with multi-lineage differentiation abilities that result from dysregulated self-renewal [3]. The cancer stem cell theory, which states that a subset of cells within a tumor have stem-like phenotypes such as self-renewal and differentiation, has introduced a novel biological paradigm for many human tumors [4, 5]. These cancer stem cells (CSCs) or tumor-initiating cells (TICs) have been proposed to cause tumor recurrence and metastasis because of their lethal characteristics, including drug resistance, invasion, and tumorigenicity [6, 7]. Therefore, the development of TIC-targeted therapy would provide new hope for cancer patients, but these treatments have not reached the clinic.

Osteosarcoma is the most common primary bone malignancy [2, 8]. Along with the development of multi-agent chemotherapy and surgical techniques including the concepts of surgical margins [9] and reconstruction [10],

patient prognosis has gradually improved over the past 30 years. However, for patients who present with metastatic disease, the outcomes are far worse, with survival rates below 30%, within 5 years of diagnosis [11]. Furthermore, some cases present with distant metastases long after the initial treatment [12]. Considering these clinical characteristics and histopathological heterogeneity, emerging reports have implicated a role for osteosarcoma TICs [13-21]. However, the molecular mechanisms underlying the phenotypes of TICs and the importance of this population in clinical situations have not been elucidated. In this study, we focused on the multiple pathways within TICs in view of microRNA (miRNA) regulation.

Emerging evidence suggests that cancer initiation and progression involve miRNAs, which are small non-coding single-stranded RNAs of 20 – 22 nucleotides that negatively regulate gene expression at the post-transcriptional level through imperfect base paring with the 3' untranslated region (UTR) of their target mRNA [22]. These miRNAs are central to RNA interference (RNAi) [23]. The biogenesis of miRNAs involves a complex protein system, including members of the Argonaute family, Pol II-dependent transcription and the RNase IIIs Drosha and Dicer [24]. Growing evidence suggests that miRNAs are involved in crucial biological processes, including development, differentiation, apoptosis and proliferation [24]. Numerous profiling studies of miRNAs have revealed that deregulation of miRNA may contribute to many types of human diseases, including cancer. Depending on the target mRNAs that they regulate, miRNAs can function as tumor promoters or suppressors, regulating the maintenance and progression of cancers and TICs [25, 26]. In addition, miRNA expression profiles have been correlated with the tumor stage, progression, and prognosis of cancer patients [27, 28]. These findings indicate that miRNAs are critical regulators of tumor development and progression.

To date, the molecular mechanisms underlying the tumor-initiating phenotypes of osteosarcoma, their clinical correlations and effective treatments against them have not been elucidated. In this study, we confirmed that the osteosarcoma $CD133^{high}$ cell population not only demonstrate a tumor-initiating phenotype but also show significant correlation with poor prognoses for osteosarcoma patients. In addition, we elucidated that miR-133a is a key regulator of cell invasion, which constitutes

these malignant phenotypes of osteosarcoma, and that silencing of miR-133a with locked nucleic acid (LNA) inhibited osteosarcoma metastasis *in vivo* when applied with current chemotherapy. Furthermore, the expression of miR-133a and its target genes significantly correlated with the prognoses of osteosarcoma patients. Thus, our preclinical trial using LNA therapeutics may represent a novel strategy for osteosarcoma treatment through regulating multiple molecular pathways of the malignant cell population within osteosarcoma.

MATERIALS AND METHODS

Osteosarcoma Cell Purification from Fresh Clinical Samples

Fresh human osteosarcoma samples were obtained in accordance with the ethical standards of the Institutional Committee on Human Experimentation from two patients who were undergoing diagnostic incisional biopsy from primary sites of osteosarcoma prior to receiving neoadjuvant chemotherapy at the National Cancer Center Hospital of Japan between October 2010 and June 2011. The osteosarcoma diagnosis and the histological subtypes were determined by certified pathologists. The surgical specimens were obtained at the time of resection and were received in the laboratory within 10 minutes, immediately mechanically disaggregated, digested with collagenase (Nitta Gelatin, Osaka, Japan, http://www.nitta-gelatin.co.jp) and washed twice with PBS. The cells were cultured in DMEM (Life Technologies, Carlsbad, CA, http://www.lifetechnologies.com) containing 10% heat-inactivated FBS (Life Technologies), penicillin (100 U/ml) and streptomycin (100 μg/ml) in 5% CO_2 in a humidified incubator at 37 °C.

Cells and Cell Culture

The human osteosarcoma cell lines SaOS2, U2OS, MG63, HOS, MNNG/HOS, and 143B were purchased from the American Type Culture Collection (ATCC, Manassas, VA, http://www.atcc.org). The human osteosarcoma cell lines HuO9 and 143B-luc were previously established in our laboratory [29, 30], and SaOS2-luc cell line, a stable luciferase-expressing cell line, was newly established using a plasmid vector. We cultured SaOS2, SaOS-luc, and HuO9 cells in RPMI 1640 (Life Technologies). U2OS, MG63, HOS, MNNG/HOS, 143B, and 143B-luc cells were cultured in DMEM (Life Technologies). All media were supplemented with 10%

heat-inactivated FBS (Life Technologies), penicillin (100 U/ml) and streptomycin (100 μg/ml). The cells were maintained under 5% CO_2 in a humidified incubator at 37 °C.

Cell Sorting and Flow Cytometry

Cell sorting by flow cytometry was performed on osteosarcoma cell lines and clinical samples using APC-conjugated monoclonal mouse anti-human CD133/2 (293C3, Miltenyi Biotec, Auburn, CA, https://www.miltenyibiotec.com) and PE-conjugated monoclonal mouse anti-human CD44 (eBioscience, San Diego, CA, http://www.ebioscience.com) antibodies. Isotype control mouse IgG2b-APC (Miltenyi Biotec) and mouse IgG2b-PE (eBioscience) served as a control. The samples were analyzed and sorted on a JSAN cell sorter (Bay Bioscience, Kobe, Japan, http://www.baybio.co.jp) and a BD FACS Aria II (BD Biosciences, Tokyo, Japan, http://www.bdj.co.jp). Viability was assessed using trypan blue exclusion. The results were analyzed using FlowJo software (Tree Star, San Carlos, CA, http://www.treestar.com).

Cell Proliferation and Cytotoxicity assays

The cell proliferation rates and cell viability were used as indicators of the relative sensitivity of the cells to doxorubicin, cisplatin, and methotrexate, and these measurements were determined using the TetraColor ONE Cell Proliferation Assay (Seikagaku, Tokyo, Japan, http://www.seikagaku.co.jp/) or Cell proliferation kit 8 (Dojindo, Kumamoto, Japan, http://www.dojindo.co.jp), according to the manufacturer's instructions. Cells growing in the logarithmic phase were seeded in 96-well plates (3×10^3 /well), allowed to attach overnight, and then treated with varying doses of doxorubicin (Sigma-Aldrich, St. Louis, MO, http://www.sigmaaldrich.com), cisplatin (Enzo Life Sciences, Farmingdale, NY, http://www.enzolifesciences.com), or methotrexate (Sigma-Aldrich) for 72 h. Triplicate wells were used for each treatment group. The absorbance was measured at 450 nm with a reference wavelength at 620 nm using EnVision (Perkin-Elmer, Waltham, MA, http://www.perkinelmer.com). The relative number of viable cells was expressed as the percent of viable cells.

Sphere Formation

Freshly isolated $CD133^{high}$ and $CD133^{low}$ osteosarcoma SaOS2 cells were plated on ultra low-attachment 96-well plates (Corning, Corning, NY, http://www.corning.com) at a concentration of a single cell per well containing 100 μl of culture medium, which

was confirmed visually. Wells containing either no cells or more than one cell were excluded for further analysis. The ratios of the wells containing spheres formed from single cells on day 10 were counted. The wells containing the cells that did not form spheres were excluded. The numbers of spheroids were counted 10 days after cell sorting. Serum-free DMEM/F12 (Life Technologies) supplemented with 20 ng/ml human recombinant EGF (Sigma-Aldrich), 10 ng/ml human recombinant bFGF (Life Technologies), 4 μg/ml insulin (Sigma-Aldrich), B27 (1:50; Life Technologies), 500 units/ml penicillin (Life Technologies) and 500 μg/ml streptomycin (Life Technologies) was used as the culture medium.

Invasion Assay

Invasion assays were performed using 24-well BD BioCoat Invasion Chambers with Matrigel (BD). A total of 1×10^5 cells were suspended in 500 μl DMEM or RPMI 1640 medium without FBS and added to the upper chamber. DMEM or RPMI 1640 medium with 10% FBS was added to the lower chamber. After incubation for 24 or 36 h, the cells on the upper surface of the filter were completely removed by wiping with cotton swabs. The filters were fixed in methanol and stained with 1% toluidine blue in 1% sodium tetraborate (Sysmex, Kobe, Japan, http://www.sysmex.co.jp). The filters were mounted onto slides, and the cells on the lower surfaces were counted.

miRNA Profiling

miRNA expression profiling was performed using a miRNA microarray manufactured by Agilent Technologies (Santa Clara, CA, http://www.home.agilent.com) that contained 866 human miRNAs. Three independently extracted RNA samples obtained from $CD133^{high}$ and $CD133^{low}$ cells just after isolation were used for the array analyses. The labeling and hybridization of the total RNA samples were performed according to the manufacturer's protocol. The microarray results were extracted using the Agilent Feature Extraction software (v10.7.3.1) and analyzed using GeneSpring GX 11.0.2 software (Agilent Technologies).

Clinical Samples for Correlating Survival with the Expression of CD133, miR-133a, and Targets of miR-133a

The osteosarcoma tissue samples were obtained from diagnostic incisional biopsies of primary osteosarcoma sites before the start of neoadjuvant chemotherapy at the National

Cancer Center Hospital of Japan between June 1997 and September 2010. We did not include patients older than 40 years of age or patients who had primary tumors located outside the extremities. Each fresh tumor sample was cut into two pieces; one piece was immediately cryopreserved in liquid nitrogen, and the other piece was fixed in formalin. The osteosarcoma diagnosis and the histological subtypes were determined by certified pathologists. Only osteosarcoma samples with the osteoblastic, chondroblastic, fibroblastic, or telangiectatic subtypes were included. The response to chemotherapy was classified as good if the tumor necrosis was 90% or greater. To correlate the survival studies with the expression of CD133 and the targets of miR-133a, 35 available cDNA samples from the cDNA library were used, and RNA from 48 available FFPE samples were used for the correlation study with miR-133a expression. The patient clinical information is summarized in Supporting Information Table S1 and S2. All patients provided written, informed consent authorizing the collection and use of their samples for research purposes. The study protocol for obtaining clinical information and collecting samples was approved by the Institutional Review Board of the National Cancer Center of Japan.

RNA Isolation and Quantitative Real-time RT-PCR of mRNAs and miRNAs

We purified total RNA from cells and tumor tissues using the miRNeasy Mini Kit (QIAGEN, Valencia, CA, http://www.qiagen.com). For qPCR of mRNAs, cDNA was synthesized using a High-Capacity cDNA Reverse Transcription Kit (Life Technologies). For each qPCR, equal amounts of cDNA were mixed with Platinum SYBR Green qPCR SuperMix (Life Technologies) and the specific primers (**Supporting Information Table S3**). We normalized gene expression levels to β-actin or GAPDH. For the qPCR of miRNAs, miRNA was converted to cDNA using the TaqMan MicroRNA Reverse Transcription Kit (Life Technologies). RNU6B small nuclear RNA was amplified as an internal control. qPCR was performed using each miRNA-specific probe included with the TaqMan MicroRNA Assay. The reactions were performed using a Real-Time PCR System 7300 with the SDS software (Life Technologies).

Transfection with Synthetic miRNAs, LNAs, and siRNAs

Synthetic hsa-miRs (Pre-miR-hsa-miR-1, 10b, 133a, and negative control (NC); Applied Biosystems, **Supporting Information Table**

S4) and locked nucleic acids (LNAs; LNA-1, 10b, 133a, and negative control; Exiqon and Gene Design, **Supporting Information Table S5**) were transfected into each cell line at 30 nM each (final concentration) using DharmaFECT 1 (GE Healthcare, Piscataway, NJ, www.gehealthcare.com). The synthetic siRNAs (Bonac Corporation, **Supporting Information Table S6**) were transfected into cells at 100 nM each (final concentration) using DharmaFECT 1 (GE Healthcare). After 24 hours of incubation, the cells were harvested and reseeded into a 6-well or 96-well plate.

Tumor Transplantation Experiments

The animal experiments in the present study were performed in compliance with the guidelines of the Institute for Laboratory Animal Research at the National Cancer Center Research Institute. Athymic nude mice or NOD/SCID mice (CLEA Japan, Tokyo, Japan, http://www.clea-japan.com) were purchased at 4 weeks of age and given at least 1 week to adapt to their new environment prior to tumor transplantation. On day 0, the mice were anesthetized with 3% isoflurane, and the right leg was disinfected with 70% ethanol. The cells were aspirated into a 1 ml tuberculin syringe fitted with a 27-G needle. The needle was inserted through the cortex of the anterior tuberosity of the tibia with a rotating movement to avoid cortical fracture. Once the bone was traversed, the needle was inserted further to fracture the posterior cortex of the tibia. A 100 μl volume of solution containing SaOS2-luc cells (10^2, 10^3, 10^4, 10^5) or 143B-luc cells (1.5×10^6) was injected while slowly removing the needle.

Monitoring Tumor Growth, Lung Metastasis, and Toxicity with/without LNA-anti-miR-133a

To evaluate LNA-133a administration to mice with spontaneous osteosarcoma lung metastases, individual mice were injected with 10 mg/kg of LNA-133a or control LNA-NC via the tail vain. LNAs were injected on days 4, 11, 18 post-inoculation with the 143B-luc cells, followed by intraperitoneum injection of 3.5 mg/kg of cisplatin on days 5, 12, 19. Each experimental condition included 10 animals per group. The development of subsequent lung metastases was monitored once per week *in vivo* using bioluminescent imaging for 3 weeks. All data were analyzed using LivingImage software (version 2.50, Xenogen, Alameda, CA). On day 22, the primary tumors and lungs of five mice in each group were resected at necropsy for weight,

bioluminescence, and histological analyses. A blood examination; weighing of the whole body, heart, liver, and skeletal muscle; and a histopathological examinations were performed for toxicity assessment. The remaining mice were observed for survival.

Comprehensive Collection and Identification of miR-133a Target mRNAs

To identify comprehensive downstream targets of miR-133a, we performed cDNA microarray profiling using two experimental approaches. First, we collected candidate genes from the cDNA microarray analysis performed on total RNA collected from SaOS2 $CD133^{low}$ cells transfected with miR-133a or NC. Second, a cDNA microarray analysis was performed on total RNA collected using anti-Ago2 antibody immunoprecipitation (Ago2-IP) from CD133low cells transduced with miR-133a or NC. The genes that were identified in the former method as downregulated with a 1.5-fold decrease and the genes identified in the latter method as upregulated with a 2.0-fold increase were defined as candidates by reference to *in silico* databases using TargetScanHuman 6.0 (http://www.targetscan.org).

Luciferase Reporter Assays

Each fragment of the 3' UTR of SGMS2 (nt 1656-1879 (binding site) of NM_152621), UBA2 (nt 2527-2654 (binding site) of NM_005499), SNX30 (nt 6659-7611 (binding site) of NM_001012944), and ANXA2 (nt 1056-1634 (binding site) of NM_001002857) were amplified and cloned into the XhoI and NotI sites of a psiCHECK-2 vector containing either the firefly or Renilla luciferase reporter gene (Promega, Tokyo, Japan, http://www.promega.co.jp). We verified all PCR products that were cloned into the plasmid using DNA sequencing to ensure that they were free of mutations and in the correct cloning direction. The primer sequences are listed in **Supporting Information Table S7**. For the luciferase reporter assay, SaOS2 cells were co-transfected with 100 ng of luciferase constructs and 100 nM synthetic miR-133a molecules or control (non-targeting siRNA oligonucleotide, QIAGEN). The firefly and Renilla luciferase activity levels were measured using the Dual-Luciferase Reporter Assay (Promega) 48 hours after transfection. The results are expressed as relative Renilla luciferase activity (Renilla luciferase/firefly luciferase).

Immunohistochemistry

To stain the miR-133a targets, we prepared slides from osteosarcoma xenograft tumors. Endogenous peroxidase was quenched with 1% H_2O_2 (30 min). The slides were heated for antigen retrieval in 10 mM sodium citrate (pH 6.0). Subsequently, we incubated the slides with monoclonal mouse anti-human SGMS2 (1:50 dilution, Abcam, Tokyo, Japan, http://www.abcam.co.jp), ANXA2 (1:250 dilution, Abcam) or isotype-matched control antibodies overnight at 4°C. Immunodetection was performed using ImmPRESS peroxidase polymer detection reagents (Vector Labs, Burlingame, CA, https://www.vectorlabs.com) and the Metal-Enhanced DAB Substrate Kit (Thermo Fisher Scientific, Yokohama, Japan, http://www.thermofisher.co.jp) in accordance with the manufacturer's directions. The sections were counterstained with hematoxylin for contrast.

Statistical Analyses

All statistical analyses were performed using SPSS Statistics Version 21 software (IBM SPSS, Tokyo, Japan, https://www.ibm.com). Student's *t* test or one-way analysis of variance (ANOVA), corrected for multiple comparisons as appropriate, was used to determine the significance of any differences between experimental groups. The differences in CD133, miR-133a, and the miR-133a targets expression among different clinicopathological data were analyzed using the chi-squared (χ^2) test or ANOVA. We carried out receiver-operating characteristic (ROC) curve analysis using the SPSS software, and the optimal cutoff points for the expression levels of CD133, miR-133a, and the target genes of miR-133a were determined by the Youden index, i.e. J = max (sensitivity + specificity – 1) [31]. The Kaplan-Meier method and the log-rank test were used to compare the survival of patients. We defined the survival period as the time from diagnosis until death, whereas living patients were censored at the time of their last follow-up. For all the analyses, we considered a p value of 0.05 or less to be significant.

RESULTS

Osteosarcoma CD133^{high} Cell Populations Are Enriched with Highly Malignant Cells with the Multiple Phenotypes

Based on the emerging evidence that tumors contain the heterogeneous cell populations, we tried to isolate the small population of highly malignant cells in osteosarcoma. In order to

evaluate the phenotypes of the cell population, we screened human osteosarcoma cell lines (SaOS2, U2OS, HOS, MG-63, HuO9, MNNG/HOS, and 143B) for the markers expressed on the highly malignant cell populations within the tumors [4, 7, 32]. As a result, we confirmed that CD133, a human structural homolog of mouse prominin-1, was expressed in a small proportion of cells ranging from 0.04% to 8.47% (**Fig. 1A, Supporting Information Fig. S1A**), which was consistent with the previous reports [18, 19]. Several examinations were performed to confirm the phenotypes of the SaOS2 $CD133^{high}$ and $CD133^{low}$ populations. Freshly isolated $CD133^{high}$ and $CD133^{low}$ osteosarcoma SaOS2 cells were plated at a concentration of a single cell and cultured immediately in a serum-free, growth factor-supplemented, anchorage-independent environment. Within 2 weeks of culture, we observed more osteosarcoma spheres from the $CD133^{high}$ cells than from the $CD133^{low}$ cells (**Fig. 1B, 1C**). The cell proliferation rate was slightly lower in $CD133^{high}$ cell population than in $CD133^{low}$ cell population (**Supporting information Fig. S1D**). To assess the difference of drug resistance, both populations were observed after exposure to doxorubicin (DOX), cisplatin (CDDP), or methotrexate (MTX), which are the standard chemotherapeutic agents that are used against osteosarcoma. The $CD133^{high}$ cells were more resistant to these chemotherapeutics than $CD133^{low}$ cells (**Fig. 1D**). In addition, $CD133^{high}$ cells showed a higher invasive ability than $CD133^{low}$ cells (**Fig. 1E, 1F**). Performing qRT-PCR reactions on mRNA from freshly isolated $CD133^{high}$ and $CD133^{low}$ cells revealed that $CD133^{high}$ SaOS2 cells expressed higher levels of *Oct3/4* and *Nanog,* which are essential transcription factors that play critical roles in the self-renewal and pluripotency of embryonic stem cells (**Fig. 1G**) [15-17]. Meanwhile, the expression levels of the genes that are essential for differentiation, such as *Runx2*, *Osterix*, and *Sox9* [33-36], were lower in $CD133^{high}$ than in $CD133^{low}$ cells (**Supporting Information Fig. S1C**). In addition, the multidrug resistance transporter genes *ABCB1*, *ABCC2*, and *ABCG2* and the metastasis-associated genes *β4-integrin*, *ezrin*, *MMP-13*, and *CXCR4* [30, 37] were upregulated in $CD133^{high}$ cells relative to $CD133^{low}$ cells (**Fig. 1G**). Importantly, the $CD133^{high}$ SaOS2 cells showed stronger tumorigenicity *in vivo* than the $CD133^{low}$ SaOS2 cells (**Fig. 1H**). We identified tumor-initiation on the right legs of 3 in 4 mice transplanted with 1×10^3 $CD133^{high}$ cells but only 1 in 4 mouse formed tumor with 1×10^3

$CD133^{low}$ cells on the left legs. To evaluate the clinical importance of CD133 expression, cell lines established from fresh human osteosarcoma biopsies were analyzed by flow cytometry, and these cell lines contained a low proportion (< 10 %) of $CD133^{high}$ cells (**Supporting Information Fig. S1B**). Furthermore, a clinical study of 35 osteosarcoma patients revealed that high expression levels of CD133 mRNA were associated with significantly worse overall survival rates among osteosarcoma patients (log-rank test, p = 0.026; **Fig. 1I, 1J, Supporting Information Figure S2A**). In this study, all biopsy samples from patients who developed lung metastasis at first diagnosis represented high expression level of CD133 (p = 0.045; **Supporting Information Table S1**), suggesting that the expression of CD133 closely correlate with osteosarcoma metastasis. Collectively, the osteosarcoma $CD133^{high}$ cell population possessed highly malignant phenotypes, and the expression of CD133 revealed a prognostic value of osteosarcoma patients.

miR-133a Functions as a Key Regulator of Malignant Phenotypes in Osteosarcoma

Following the confirmation of the malignant phenotypes in the osteosarcoma $CD133^{high}$ population, we further characterized the molecular mechanisms underlying these phenotypes. We focused on miRNAs because of their ability to simultaneously regulate multiple pathways responsible for the malignant phenotypes by targeting multiple genes. miRNAs are small, regulatory RNA molecules that modulate the post-transcriptional expression of their target genes and play important roles in a variety of physiological and pathological processes, including tumor biology [23, 25, 38]. miRNA expression profiling has become a useful diagnostic and prognostic tool, and many studies have indicated that miRNAs act as either oncogenes or tumor suppressors [38]. In our miRNA microarray analysis of isolated $CD133^{high}$ and $CD133^{low}$ cells using 866 sequence-validated human miRNAs, we identified 20 miRNAs that were upregulated in $CD133^{high}$ cells and additional qRT-PCR analysis demonstrated that the expression levels of miR-1 and miR-10b, together with miR-133a, which represents the 'miR-1 cluster' transcribed from adjacent miR-1 genes, were consistent with the microarray data (**Fig. 2A, Supporting Information Fig. S3A, Table S8**). Indeed, miR-1 and miR-133a are physically linked, and both the miR-1-1/miR-133a-2 (chromosome 20q13.33)

as well as miR-1-2/miR-133a-1 clusters (chromosome 18q11.2) are present. miR-10b is embedded in the *HOX* gene cluster and maps between the *HOXD3* and *HOXD4* genes on chromosome 2q31. Since miR-10a and miR-133b would presumably be functionally redundant to miR-10b and miR-133b respectively, we also confirmed that miR-133b, but not miR-10a, was upregulated in $CD133^{high}$ cell population (**Supporting Information Fig. S3B**).

To determine whether these miRNAs could regulate the malignant phenotypes of osteosarcoma, we manipulated the expression levels of miR-1, 10b, and 133a in $CD133^{low}$ cells (**Supporting Information Fig. S4A**). These miRNAs, especially miR-133a, enhanced the invasiveness of $CD133^{low}$ cells compared with control oligos (**Fig. 2B, 2C**). Interestingly, the combined transfection of all of these miRNAs enhanced the invasiveness of $CD133^{low}$ cells to the greatest extent (**Fig. 2C**). However, the transfection of miR-133a did not increase the mRNA level of CD133 (**Supporting Information Fig. S4B**), suggesting that miR-133a does not affect the expression of the molecules upstream of CD133. These results indicated that miR-133a simultaneously regulate several molecular pathways that are associated with cell invasion of the malignant cell population within osteosarcoma. In our experiment using fresh clinical samples, miR-133a expression was also high in the $CD133^{high}$ fraction of osteosarcoma biopsies (**Fig. 2D**). Surprisingly, a clinical study based on qRT-PCR using clinical formalin-fixed paraffin-embedded (FFPE) samples revealed that the high expression of miR-133a closely correlated with a poor prognosis of osteosarcoma patients (log-rank test, $p = 0.032$ for overall survival, $p = 0.081$ for disease-free survival; **Fig. 2E, 2F, Supporting Information Figure S2B, Table S2**).

Silencing of miR-133a Inhibits the Cell Invasion of $CD133^{high}$ Osteosarcoma Cell Population

To evaluate whether silencing of miR-133a show the therapeutic effect on osteosarcoma cells, we manipulated the expression of miR-133a by introducing locked nucleic acids (LNAs). LNAs are a class of nucleic acid analogs that possess a very high affinity and excellent specificity toward complementary DNA and RNA, and LNA oligonucleotides have been applied as antisense molecules both *in vitro* and *in vivo* [39-41]. The SaOS2 $CD133^{high}$ cell population was isolated by cell

sorting and was then transfected with LNA-anti-miR-133a (LNA-133a) and LNA-negative control (LNA-NC). As a control, the isolated SaOS2 $CD133^{low}$ cell population was also transfected with LNA-NC. Prior to functional assay, we confirmed the efficacy of LNA-133a using both qRT-PCR analysis and a sensor vector which allowed us to measure the suppressive effect of LNA by luciferase assay (**Supporting Information Fig. S5A-D**). We observed that the LNA-133a-treated SaOS2 $CD133^{high}$ cells demonstrated decreased invasiveness relative to LNA-NC-treated $CD133^{high}$ cells, whereas there was no significant difference of cell proliferation between the two populations (**Fig. 2G, 2H, Supporting Information Fig. 5E**). These observations suggest that silencing of miR-133a in $CD133^{high}$ cells could reduce the cell invasion of the malignant cell population within osteosarcoma tissue.

The Expression Levels of miR-133a in Osteosarcoma Cells are Enhanced by Chemotherapy

Next, we validated the efficacy of LNA-133a on highly malignant metastatic osteosarcoma 143B cells, since SaOS2 cells represent low metastatic ability *in vivo* [42, 43]. Meanwhile, we needed to evaluate the efficacy of LNA on 'bulk' 143B cells, assuming clinical situations. As a result, LNA-133a reduced the invasiveness of 143B cells (**Fig. 3A, 3B**), but did not influence cell proliferation (**Supporting Information Fig. 5F**). Since recent study has indicated a novel mechanism of chemotherapy-induced tumor progression via expansion of TIC population [44], the expression levels of CD133 and the related miR-133a within cells treated with or without chemotherapeutics were analyzed. As a result, we observed that the expression levels of miR-133a, together with CD133, were enhanced by chemotherapy. qRT-PCR analysis revealed that DOX-treated or CDDP-treated (2 days) 143B cells expressed higher levels of CD133 and miR-133a compared with untreated 143B cells (**Fig. 3C, 3D**). Therefore, silencing of miR-133a before or during chemotherapy may prevent the increased expression of miR-133a, which enhanced the malignant phenotypes and was induced by chemotherapeutics.

Therapeutic Administration of LNA-anti-miR-133a with Chemotherapy Inhibits Spontaneous Lung Metastasis and Prolongs the Survival of Osteosarcoma-bearing Mice

To extend our *in vitro* findings and to determine whether silencing of miR-133a could be an effective therapeutic option for osteosarcomas, we next examined the effect of LNA-133a on a spontaneous lung metastasis model of osteosarcoma. Experimentally, 1.5 x 10^6 143B cells transfected with the firefly luciferase gene (143B-luc) were implanted orthotopically into the right proximal tibia of athymic nude mice. The implanted tumor growth and the presence of distant metastases were analyzed weekly for luciferase bioluminescence using an *in vivo* imaging system (IVIS). We used a new treatment protocol (**Fig. 4A**) with the intravenous (i.v.) administration of LNA-133a (10 mg/kg) 24 h before intraperitoneal (i.p.) injection of cisplatin (3.5 mg/kg) to prevent the induction of malignant phenotypes by chemotherapy, which were indicated in the *in vitro* experiments. Prior to conducting these animal studies, we confirmed that miR-133a levels were reduced in osteosarcoma tissues from LNA-133a-treated mice compared with control mice (**Supporting Information Fig. S6A, S6B**). To assess the efficacy of our protocol, the results were compared with the results obtained for the following four control groups (n = 10 per group): the control saline followed by control saline group, the LNA-NC followed by control saline group, the LNA-133a followed by control saline group, and the LNA-NC followed by cisplatin group. After implantation of the 143B-luc cells, five mice within each one cage were sacrificed at 3 weeks after evaluating lung metastasis by *in vivo* imaging and validated for lung metastasis formation by additional *in vivo* imaging and histological examination of the lung, whereas the other five mice in the other cage were evaluated for survival periods. The results demonstrated that the tumor expression levels of miR-133a were decreased in the presence of LNA-133a (**Fig. 4B**). Although tumor growth at the primary site was significantly reduced in cisplatin-treated group, we identified no significant difference between LNA-133a-cisplatin-treated mice and LNA-NC-cisplatin-treated mice (**Fig. 4C, 4D**). We observed lung metastases on day 22 in 9 (90%) saline-saline-treated mice, 8 (80%) LNA-NC-saline-treated mice, 7 (70%) LNA-133a-saline-treated mice, 8 (80%) LNA-NC-CDDP-treated mice, and 3 (30%) LNA-133a-CDDP-treated mice (n = 10; **Fig.**

4E, 4F). We validated the signal intensity of lung luminescence and observed the decreased signal intensity chest lesion of LNA-133a-CDDP-treated mice compared to lung from LNA-NC-CDDP-treated mice (**Fig. 4G**). Both the number and size of lung metastases were validated by histopathological examination (**Fig. 4H**). We found low cell concentration in lung metastatic foci of cisplatin-treated groups, indicating therapeutic effect of chemotherapy, and identified smallest number of osteosarcoma metastatic foci in the lung of LNA-133a-cisplatin-treated mice. Furthermore, LNA-133a-CDDP-treated mice showed longest survival periods among the five groups in Kaplan-Meier analysis (log-rank test, $p = 0.026$; **Fig. 4I**). Despite the conserved sequence of mature hsa-miR-133a and mmu-miR-133a (**Supporting Information Fig. S7A**), all mice exhibited minimal toxic effects on various tissues, including the heart, liver, skeletal muscle, and blood test, during the observation period (**Supporting Information Fig. S7B–S7H, Supporting Information Fig. S8A–S8I**). Thus, systemic administration of LNA-133a was effective for the suppression of lung metastases in a xenograft model of a highly metastatic osteosarcoma in the presence of cisplatin.

Multiple Target Genes of miR-133a Function as Regulators of Cell Invasion and Closely Correlate with Clinical Behavior of Osteosarcoma

We demonstrated that miR-133a regulated the malignancy of $CD133^{high}$ osteosarcoma cell population and that silencing of miR-133a expression with chemotherapeutics inhibited the osteosarcoma metastasis *in vivo*. Next, to understand the molecular mechanism regulated by miR-133a in the tumor-initiating population, we performed mRNA expression profiling using two different microarray analyses together with *in silico* predictions (Supporting **Information Fig. S9A**). We detected 1812 genes that were downregulated by least 1.2-fold in the first microarray analysis, which was performed from total RNA collected from SaOS2 $CD133^{low}$ cells transduced with miR-133a or NC. Furthermore, 4976 genes were upregulated by at least 2.0-fold in the second microarray analysis of mRNA expression using RNA collected using anti-Ago2 antibody immunoprecipitation (Ago2 IP) in $CD133^{low}$ cells transduced with miR-133a or NC. Subsequently, 226 genes were collected using both methods, and 20 genes were identified in TargetScanHuman 6.0, a publicly available *in silico* database (**Fig. 5A**). Overall, 10 putative miR-133a target genes

were selected from these combined data, and we reduced the expression of these molecules using an siRNA-induced gene knockdown system to investigate whether these candidates are functionally important targets of miR-133a in osteosarcoma cells. As a result, the knockdown of four genes (*SGMS2*, *UBA2*, *SNX30*, and *ANXA2*) enhanced the invasiveness of $CD133^{low}$ SaOS2 cells (**Fig. 5B**). To validate whether these molecules are regulated by miR-133a, we cloned the 3' UTR fragment (**Fig. 5C**) containing the putative miR-133a binding sites downstream of a luciferase coding sequence and performed co-transfection of the luciferase reporter and miR-133a oligos in SaOS2 cells. Luciferase activity levels were reduced by approximately 36 – 55 % in the cells co-transfected with miR-133a compared with the cells co-transfected with the NC oligos (**Fig. 5D**). Consequently, *SGMS2*, *UBA2*, *SNX30*, and *ANXA2* functioned as direct targets of miR-133a. Indeed, these molecules have been suggested to have anti-tumor function in the other types of tumors [45-47]. Among them, *ANXA2* is downregulated in osteosarcoma metastases compared to primary site [48]. The expression levels of these targets were decreased in $CD133^{high}$ cells (**Supporting Information Fig. S9B**) and reduced via miR-133a upregulation in $CD133^{low}$ cells (**Supporting Information Fig. S9C**). The increased expression levels of the targets after silencing of miR-133a were confirmed by immunohistochemistry of LNA-treated tumors and qRT-PCR (**Fig. 5E,F and Supporting Information Fig. S9D**). Taken together, LNA-133a was found to inhibit cell invasion of the malignant cell population of osteosarcoma through multiple molecular pathways. Finally, we observed a strikingly close correlation between these mRNA expression levels of the miR-133a targets and osteosarcoma patient prognosis (**Fig. 6A-6D**). Patients with higher expression levels of these targets significantly survived longer than those with lower expression levels. These results would support the importance of regulating the expression of miR-133a during current osteosarcoma treatment, providing insight into the development of more effective therapies against osteosarcoma.

DISCUSSION

Cancer researchers today are confronted with how to overcome the natural resistance and the acquired resistance of cancer cells within tissue, despite the many cancer treatment options. The

CSC or TIC hypothesis has been an attractive model to account for the functional heterogeneity that is commonly observed in solid tumors [7]. To characterize and eliminate the malignant cells in cancers that follow this model, it has been necessary to focus on the small subpopulations of tumorigenic cells [49]. Tremendous efforts and evidence have accumulated to identify these subpopulations [13-18, 20, 21]. However, these markers are generally difficult to be targeted because of their distribution on the normal stem cells. For example, targeting CD133 seems unsafe because this cell-surface protein is primarily expressed in stem and progenitor cells [50] such as the embryonic epithelium [51], brain stem cells [52], and hematopoietic stem cells [32, 53]. Therefore, the molecular mechanisms underlying the malignant phenotypes must be elucidated to avoid toxicities, which have not been fully accomplished. On the basis of our results, we propose novel therapeutic strategies, beyond the use of traditional antiproliferative agents, for suppression of the highly malignant cell population within osteosarcoma using RNAi therapeutics, which is expected to be the "next-generation" anti-cancer strategy. Subsequently, we present four novel discoveries that were identified in a preclinical trial of novel therapeutic strategies against osteosarcoma.

First, we identified human miR-133a as a key regulator of the malignant tumor-initiating phenotypes of osteosarcoma. The other miRNAs that might regulate these phenotypes included miR-1 and miR-10b. The human miRNA hsa-miR-10b is also positively associated with high-grade malignancies, including breast cancer [54, 55], pancreatic adenocarcinomas [56] and glioblastomas [57]. However, the importance of miR-10b in sarcoma development has not been previously reported. In our experiment, miR-10b regulated, less than miR-133a, the cell invasion of osteosarcoma. The human miRNAs hsa-miR-1 and hsa-miR-133a are located on the same chromosomal region in a so-called cluster. We found that miR-1 showed only a little efficacy on invasiveness in osteosarcoma cells. The most important miRNA that could regulate the multiple phenotypes of osteosarcoma-initiating cells was miR-133a. Although miR-1 and miR-133a correlate with the proliferation of muscle progenitor cells and promote myogenesis [58], their importance in muscle physiology and disease remains unclear [59]. Indeed, miR-133a may be dispensable for the normal development and function of skeletal